AMERICAN SOCIETY FOR MICROBIOLOGY | Infection and Immunity®

HOST RESPONSE AND INFLAMMATION

Arginase-1 Expression in Myeloid Cells Regulates *Staphylococcus aureus* Planktonic but Not Biofilm Infection

Kelsey J. Yamada,[a] Cortney E. Heim,[a] Amy L. Aldrich,[a] Casey M. Gries,[a]* Anna G. Staudacher,[a]* Tammy Kielian[a]

[a]Department of Pathology and Microbiology, University of Nebraska Medical Center, Omaha, Nebraska, USA

ABSTRACT *Staphylococcus aureus* is a leading cause of device-associated biofilm infections, which represent a serious health care concern based on their chronicity and antibiotic resistance. We previously reported that *S. aureus* biofilms preferentially recruit myeloid-derived suppressor cells (MDSCs), which promote monocyte and macrophage anti-inflammatory properties. This is associated with increased myeloid arginase-1 (Arg-1) expression, which has been linked to anti-inflammatory and profibrotic activities that are observed during *S. aureus* biofilm infections. To determine whether MDSCs and macrophages utilize Arg-1 to promote biofilm infection, Arg-1 was deleted in myeloid cells by use of *Tie-2*^{Cre} mice. Despite Arg-1 expression in biofilm-associated myeloid cells, bacterial burdens and leukocyte infiltrates were similar between wild-type (WT) and *Arg-1*$^{fl/fl}$;*Tie-2*^{Cre} conditional knockout (KO) mice from days 3 to 14 postinfection in both orthopedic implant and catheter-associated biofilm models. However, inducible nitric oxide synthase (iNOS) expression was dramatically elevated in biofilm-associated MDSCs from *Arg-1*$^{fl/fl}$;*Tie-2*^{Cre} animals, suggesting a potential Arg-1-independent compensatory mechanism for MDSC-mediated immunomodulation. Treatment of *Arg-1*$^{fl/fl}$;*Tie-2*^{Cre} mice with the iNOS inhibitor N6-(1-iminoethyl)-L-lysine (L-NIL) had no effect on biofilm burdens or immune infiltrates, whereas treatment of WT mice with the Arg-1/ornithine decarboxylase inhibitor difluoromethylornithine (DFMO) increased bacterial titers, but only in the surrounding soft tissues, which possess attributes of a planktonic environment. A role for myeloid-derived Arg-1 in regulating planktonic infection was confirmed using a subcutaneous abscess model, in which *S. aureus* burdens were significantly increased in *Arg-1*$^{fl/fl}$;*Tie-2*^{Cre} mice compared to those in WT mice. Collectively, these results indicate that the effects of myeloid Arg-1 are context dependent and are manifest during planktonic but not biofilm infection.

KEYWORDS arginase-1, biofilm, *S. aureus*, macrophage, myeloid-derived suppressor cell

Staphylococcus aureus is a leading cause of community-acquired and nosocomial infections in humans (1–7), and the presence of foreign materials increases infection risk due to the ability of *S. aureus* to form biofilms (3, 8, 9). Biofilms are heterogeneous bacterial communities that are difficult to eradicate because of their chronicity and recalcitrance to antibiotic therapy (3, 8, 9). In addition, previous work from our laboratory has shown that *S. aureus* biofilms actively skew the host immune response toward an anti-inflammatory phenotype that is characterized by the preferential recruitment of myeloid-derived suppressor cells (MDSCs) and anti-inflammatory monocytes and macrophages, whereas neutrophils and T cell infiltrates are less abundant (10–15). MDSCs recruited to the site of biofilm infection express interleukin-10 (IL-10), which is one contributing mechanism of immune suppression (12). In addition, biofilm-associated MDSCs and macrophages upregulate arginase-1 (Arg-1) expression, suggest-

Received 20 March 2018 **Accepted** 9 April 2018

Accepted manuscript posted online 16 April 2018

Citation Yamada KJ, Heim CE, Aldrich AL, Gries CM, Staudacher AG, Kielian T. 2018. Arginase-1 expression in myeloid cells regulates *Staphylococcus aureus* planktonic but not biofilm infection. Infect Immun 86:e00206-18. https://doi.org/10.1128/IAI.00206-18.

Editor Victor J. Torres, New York University School of Medicine

Address correspondence to Tammy Kielian, tkielian@unmc.edu.

* Present address: Casey M. Gries, Division of Biomedical Sciences, University of California at Riverside Medical School, Riverside, California, USA; Anna G. Staudacher, Northwestern University Feinberg School of Medicine, Chicago, Illinois, USA.

ing that Arg-1 may further potentiate the anti-inflammatory and profibrotic cellular responses that are favored during *S. aureus* biofilm infections (10, 16, 17).

Arg-1 catalyzes the hydrolysis of arginine to ornithine and urea (18). During an immune response, myeloid-derived Arg-1 is an important enzyme involved in the regulation of arginine availability (18–22), and previous studies have demonstrated that myeloid-derived Arg-1 can inhibit proinflammatory immune responses (18, 23–27). Arginine is a substrate for both Arg-1 and inducible nitric oxide synthase (iNOS), which are characteristic markers of anti- and proinflammatory macrophages, respectively (24, 28–30). In myeloid cells, ornithine generation by Arg-1 is used for proline or polyamine synthesis through ornithine decarboxylase (ODC), which promotes fibrosis by collagen formation (18). A previous study demonstrated the importance of host-derived polyamines for *S. aureus* clearance and wound healing in a subcutaneous (s.c.) abscess model that represents planktonic infection (31); however, a role for Arg-1 action in the context of biofilms has not yet been explored. Biofilm infections are often encompassed by a fibrotic response, which coincides with robust Arg-1 expression (10, 15, 16). Arg-1 activity also inhibits NO-mediated killing of pathogens by macrophages, since arginine is the primary substrate for iNOS (28–30). Furthermore, extracellular arginine depletion leads to reduced CD3ζ chain expression and the inability to augment cyclin D3 and cdk4, leading to T cell hyporesponsiveness and cell cycle arrest, respectively (19–23, 26, 32). However, the effects of MDSC Arg-1 on inhibition of T cell proliferation may be context dependent, as some studies have not demonstrated a role for the enzyme (33, 34). Previous work reported that myeloid-derived Arg-1 expression has a pathological role in several cancers, Alzheimer's disease, and bacterial and helminth infections, establishing it as a key enzyme in dictating disease pathogenesis and immune outcomes (18, 24, 35, 36). Therefore, elevated Arg-1 expression by MDSCs and/or macrophages may participate in preventing an effective immune response to *S. aureus* biofilm infection through the depletion of extracellular arginine and suppression of proinflammatory responses.

The objective of the present study was to examine the functional role of myeloid-derived Arg-1 in promoting device-associated *S. aureus* biofilm infection. Using conditional knockout (KO) mice to delete Arg-1 in myeloid cells (*Arg-1*$^{fl/fl}$;*Tie-2*^{Cre} mice) (24, 37), we established that Arg-1 expression was significantly reduced in myeloid cells *in vitro* and in MDSCs and macrophages isolated from *S. aureus* biofilm infections *ex vivo*. Utilizing two device-associated *S. aureus* biofilm infection models, we found that bacterial burdens were not dramatically different between wild-type (WT) and *Arg-1*$^{fl/fl}$;*Tie-2*^{Cre} myeloid conditional KO mice. Further investigation showed that MDSCs from *Arg-1*$^{fl/fl}$;*Tie-2*^{Cre} conditional KO animals had upregulated iNOS expression, suggesting a possible compensatory mechanism for arginine depletion and immunomodulation. However, treatment of *Arg-1*$^{fl/fl}$;*Tie-2*^{Cre} mice with a small-molecule inhibitor of iNOS did not affect *S. aureus* biofilm burdens or leukocyte infiltrates. Additive effects were also not observed when mice were treated with a small-molecule inhibitor of NADPH oxidase. However, in the orthopedic implant model, treatment of WT mice with the arginase and ODC inhibitor difluoromethylornithine (DFMO) increased bacterial titers, but only in the surrounding soft tissue, which possesses some attributes of a planktonic environment, not in the joint and femur, which model biofilm growth. Indeed, a role for myeloid-derived Arg-1 in regulating planktonic infection was confirmed using a subcutaneous abscess model in which *S. aureus* burdens were significantly increased in *Arg-1*$^{fl/fl}$;*Tie-2*^{Cre} mice compared to those in WT animals. Collectively, these results demonstrate that myeloid-derived Arg-1 controls *S. aureus* growth during planktonic but not biofilm growth *in vivo*. By extension, the lack of Arg-1 involvement during biofilm formation represents another immune evasion mechanism leading to infection persistence.

RESULTS

Arginase-1 expression and enzyme activity are significantly reduced in myeloid cells from Arg-1 conditional KO mice. Arginase-1 is a marker of anti-inflammatory macrophages and inhibits inflammatory responses through depletion of

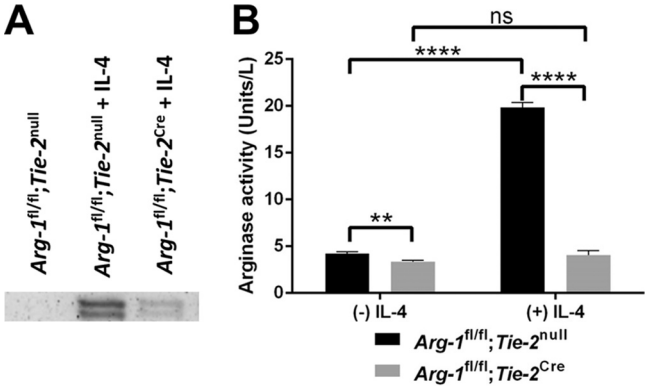

FIG 1 Arginase-1 expression and enzymatic activity are significantly reduced in *Arg-1*$^{fl/fl}$;*Tie-2*^{Cre} bone marrow-derived macrophages. Bone marrow-derived macrophages were left unstimulated or treated with rmIL-4 (10 ng/ml) for 24 h, whereupon whole-cell protein extracts (20 μg) were used for Western blotting (A) and arginase activity assays (B). Arginase activity in whole-cell extracts was measured by the amount of enzyme that converted 1.0 μmol of L-arginine to ornithine and urea per minute. ns, not significant; **, $P < 0.01$; ****, $P < 0.0001$ (one-way ANOVA with Bonferroni's multiple-comparison test).

available arginine stores (18, 22, 24, 35, 38, 39). Our laboratory previously reported increased Arg-1 expression in MDSCs, monocytes, and macrophages infiltrating tissues surrounding an *S. aureus* biofilm infection (10, 12–14, 16). Although MDSC depletion improved biofilm clearance by enhancing monocyte proinflammatory activity (12, 14), the mechanism of action and whether Arg-1 was involved remained unclear. This was an important issue to address, since Arg-1 activity has been implicated in several types of cancers, Alzheimer's disease, and infection (18, 24, 35, 36). In the current study, we used two mouse models of device-associated *S. aureus* biofilm infection to determine the role of myeloid-derived Arg-1 in shaping leukocyte infiltrates and promoting biofilm persistence. Prior reports demonstrated that LysM-driven expression of Cre recombinase is inefficient at flox-mediated Arg-1 deletion (24, 40). This was confirmed in the current study, where significant Arg-1 activity remained in *Arg-1*$^{fl/fl}$;*LysM*^{Cre} macrophages compared to that in wild-type cells (see Fig. S1 in the supplemental material). As an alternative approach, we utilized *Arg-1*$^{fl/fl}$;*Tie-2*^{Cre} mice, which have been shown to efficiently delete Arg-1 from myeloid cells (24). We first confirmed efficient Arg-1 deletion in myeloid cells from *Arg-1*$^{fl/fl}$;*Tie-2*^{Cre} conditional KO mice. Both Arg-1 expression and enzyme activity were significantly increased in wild-type *Arg-1*$^{fl/fl}$;*Tie-2*^{null} macrophages in response to IL-4 (Fig. 1A and B). In contrast, bone marrow-derived macrophages from *Arg-1*$^{fl/fl}$;*Tie-2*^{Cre} mice displayed significant decreases in Arg-1 expression and activity relative to those in *Arg-1*$^{fl/fl}$;*Tie-2*^{null} control cells, both at baseline and following IL-4 treatment, confirming effective gene deletion (Fig. 1A and B). Arginase activity in *Arg-1*$^{fl/fl}$;*Tie-2*^{Cre} macrophages may result from mitochondrial Arg-2 expression that can also catalyze the substrate used for the arginase assay (41).

Myeloid-derived arginase-1 does not dramatically affect *S. aureus* device-associated biofilm infection. Based on our *in vitro* studies demonstrating that Arg-1 activity was significantly reduced in *Arg-1*$^{fl/fl}$;*Tie-2*^{Cre} conditional KO macrophages, we next examined the role of Arg-1 in the establishment and persistence of *S. aureus* biofilms by using two infection models. The first was an orthopedic implant-associated biofilm infection model, which our laboratory has shown is dominated by MDSCs that express Arg-1 and monocytes polarized toward an anti-inflammatory state (12–14). No significant differences in biofilm burdens or leukocyte infiltrates were observed between *Arg-1*$^{fl/fl}$;*Tie-2*^{Cre} conditional KO and *Arg-1*$^{fl/fl}$;*Tie-2*^{null} mice over the 2-week infection period (Fig. 2). We next examined a mouse model of catheter-associated biofilm infection, which is typified by more robust macrophage infiltrates, fibrotic responses, and Arg-1 expression than those in the orthopedic implant model (10, 15). Although MDSC infiltrates and bacterial burdens were significantly increased in catheter-associated tissues of *Arg-1*$^{fl/fl}$;*Tie-2*^{Cre} conditional KO mice at day 10 postinfection (Fig. 3), this did not

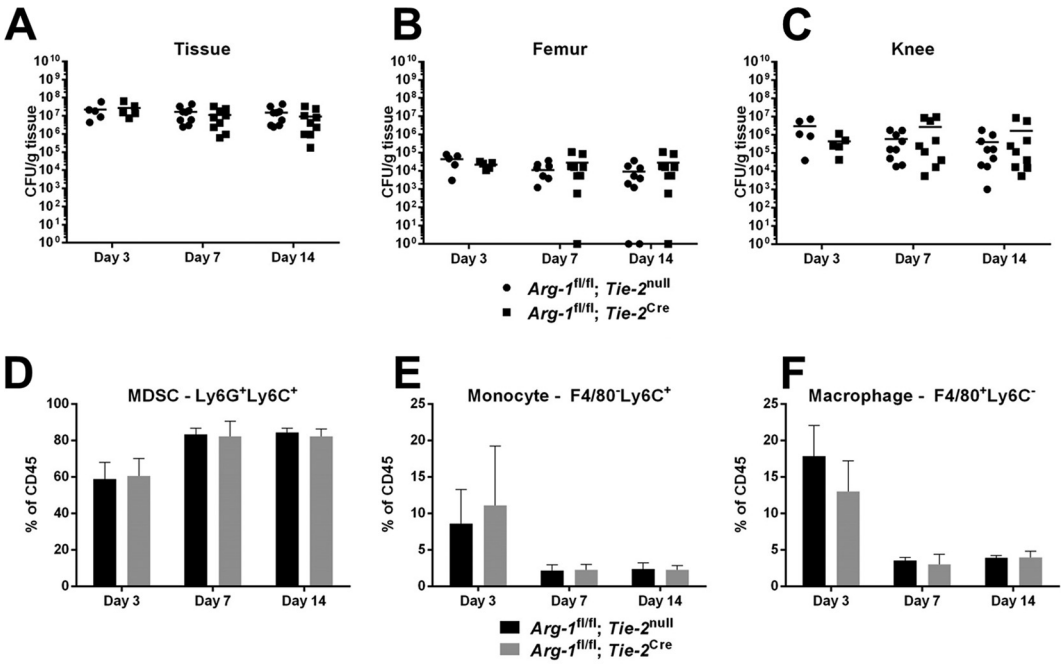

FIG 2 Arginase-1 expression in myeloid cells does not influence *S. aureus* orthopedic implant infection. Titanium orthopedic implants were placed in the femurs of *Arg-1*$^{fl/fl}$;*Tie-2*^{null} (WT) and *Arg-1*$^{fl/fl}$;*Tie-2*^{Cre} mice and inoculated with 10^3 CFU *S. aureus* LAC. (A to C) Tissues surrounding infected implants, femurs, and knee joints were collected at the indicated intervals postinfection to quantify bacterial burdens. (D to F) Infiltrating leukocyte populations in implant-associated tissues were evaluated by flow cytometry. (D) MDSCs; (E) monocytes; (F) macrophages. Results are representative of two independent experiments.

dramatically alter biofilm growth at later time points (days 14 to 28) (data not shown). No significant differences in arginase activity were observed in either tissue or femur homogenates from WT and *Arg-1*$^{fl/fl}$;*Tie-2*^{Cre} mice in the orthopedic implant model (Fig. S2). This is likely because fibroblasts and other stromal cells outnumber myeloid cells in these compartments and contribute to the arginase pool at the site of infection. In addition, we did not observe any dramatic alterations in tissue integrity and collagen content as determined by hematoxylin and eosin (H&E) and trichrome staining, respectively (data not shown). As a quantitative means to assess collagen formation, a hydroxyproline assay was performed. Although hydroxyproline levels were elevated at day 3 postinfection in *Arg-1*$^{fl/fl}$;*Tie-2*^{Cre} mice in the catheter-associated infection model (Fig. S3), this was not observed at later time points, which confirmed the similarities in collagen levels between the two strains. Collectively, these results indicate that although Arg-1 expression is increased at the site of *S. aureus* biofilm infection, the enzyme itself in myeloid cells is not critical for regulating biofilm growth.

iNOS expression is increased in biofilm-associated MDSCs from *Arg-1*$^{fl/fl}$;*Tie-2*^{Cre} conditional KO mice. To establish that the overall lack of differences between *Arg-1*$^{fl/fl}$;*Tie-2*^{Cre} myeloid conditional KO and *Arg-1*$^{fl/fl}$;*Tie-2*^{null} mice in both the catheter and orthopedic implant infection models was not due to inefficient Arg-1 deletion *in vivo*, Arg-1 expression was examined in myeloid cells recovered from the site of infection. Both MDSCs ($CD45^+$ $Ly6G^{high}$ $Ly6C^+$) and monocytes ($CD45^+$ $Ly6G^-$ $Ly6C^+$) were isolated by fluorescence-activated cell sorter (FACS) analysis from *Arg-1*$^{fl/fl}$;*Tie-2*^{Cre} and *Arg-1*$^{fl/fl}$;*Tie-2*^{null} control mice at days 7 and 14 postinfection, whereupon Arg-1 expression and activity were assessed by reverse transcription-quantitative PCR (RT-qPCR) and enzymatic assays, respectively (Fig. 4). As expected, Arg-1 expression and activity were dramatically reduced in macrophages and MDSCs from *Arg-1*$^{fl/fl}$;*Tie-2*^{Cre} conditional KO mice compared to those in cells from *Arg-1*$^{fl/fl}$;*Tie-2*^{null} controls in the catheter-associated infection model at days 7 and 14 (Fig. 4A). Because myeloid conditional Arg-1 deletion was verified in this model, this analysis was not repeated

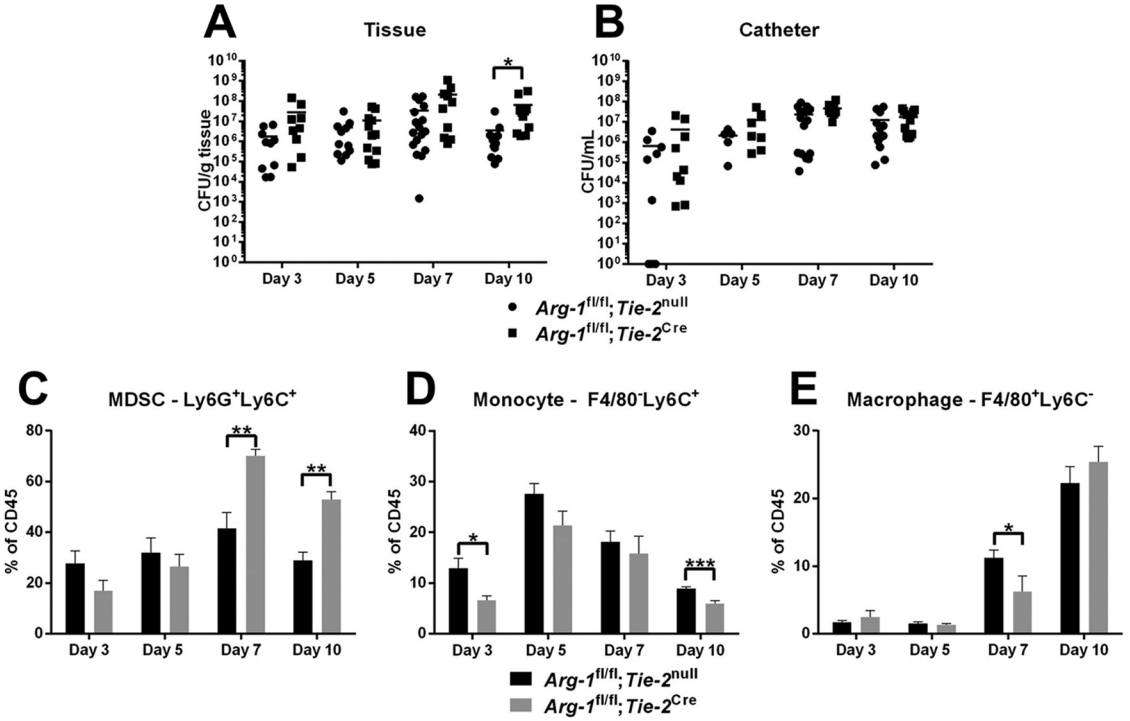

FIG 3 Arginase-1 in myeloid cells does not dramatically affect *S. aureus* catheter-associated biofilm infection. Catheter-associated infections were established in *Arg-1*$^{fl/fl}$;*Tie-2*^{null} (WT) and *Arg-1*$^{fl/fl}$;*Tie-2*^{Cre} mice following challenge with 10^3 CFU of *S. aureus* LAC. Animals were sacrificed at the indicated intervals postinfection, whereupon bacterial burdens in the surrounding tissue (A) and catheter (B) were determined and infiltrating leukocyte populations evaluated by flow cytometry (C to E). Results are representative of three independent experiments. *, $P < 0.05$; **, $P < 0.01$; ***, $P < 0.001$ (unpaired 2-tailed Student's *t* test).

with the orthopedic implant biofilm model. Interestingly, MDSCs from *Arg-1*$^{fl/fl}$;*Tie-2*^{Cre} myeloid conditional KO mice showed a dramatic increase in iNOS expression (Fig. 4A). Since prior studies from our laboratory revealed a critical role for MDSCs in attenuating monocyte/macrophage proinflammatory activity and promoting biofilm persistence (12, 14), this suggested that a potential compensatory mechanism for arginine depletion may exist via upregulation of iNOS by MDSCs in the absence of Arg-1.

iNOS or ROS do not compensate for arginase-1 deficiency in myeloid cells. Given the observed increase in iNOS expression in MDSCs from Arg-1 myeloid conditional KO mice, we treated *Arg-1*$^{fl/fl}$;*Tie-2*^{Cre} animals with N6-(1-iminoethyl)-L-lysine (L-NIL), a small-molecule inhibitor with selectivity for iNOS (cytokine inducible) over

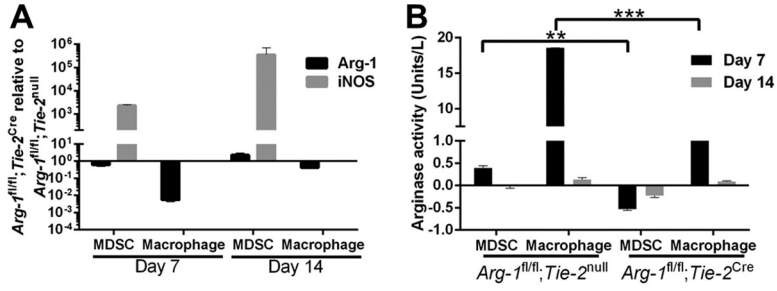

FIG 4 MDSCs and macrophages from *Arg-1*$^{fl/fl}$;*Tie-2*^{Cre} mice express limited arginase-1 *in vivo*. Catheter-associated infections were established in *Arg-1*$^{fl/fl}$;*Tie-2*^{null} (WT) and *Arg-1*$^{fl/fl}$;*Tie-2*^{Cre} mice following challenge with 10^3 CFU of *S. aureus* LAC. Animals were sacrificed at days 7 and 14 postinfection, whereupon MDSCs ($CD45^+$ $Ly6G^{high}$ $Ly6C^+$) and monocytes ($CD45^+$ $Ly6G^-$ $Ly6C^+$) were isolated by FACS analysis for RT-qPCR quantification of Arg-1 and iNOS expression (A) and arginase activity assay (B). Results are representative of two independent experiments. **, $P < 0.01$; ***, $P < 0.001$ (unpaired 2-tailed Student's *t* test).

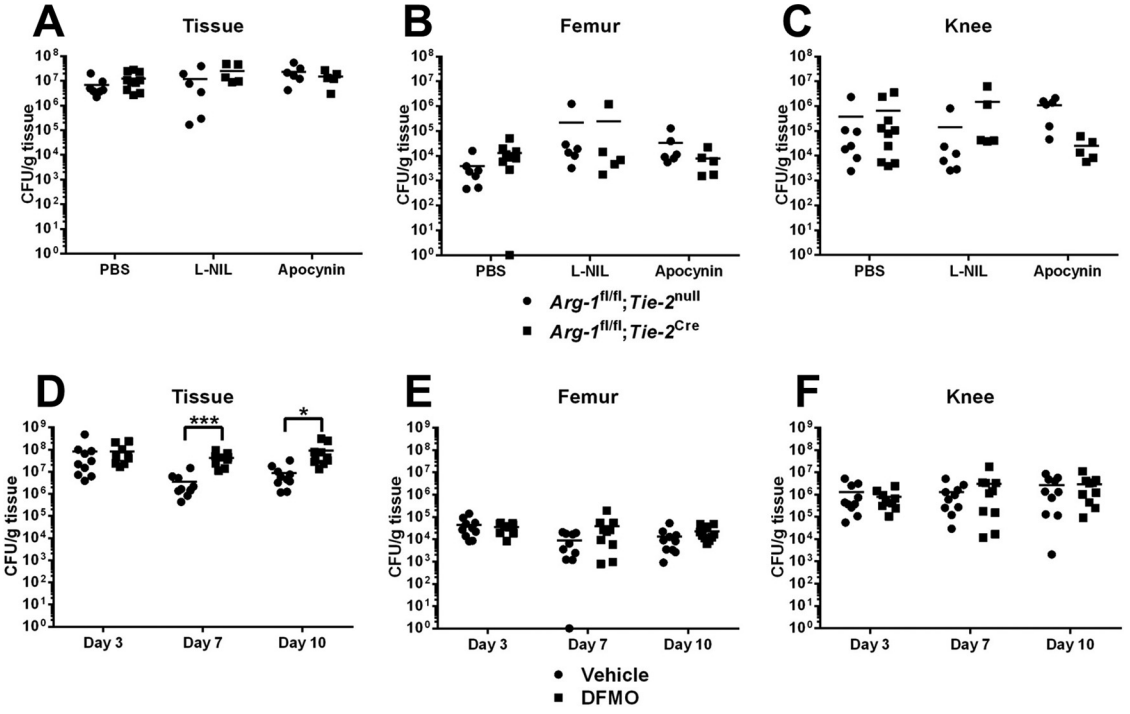

FIG 5 iNOS or reactive oxygen species do not compensate for arginase-1 deficiency in myeloid cells. *S. aureus* orthopedic implant infections were established in *Arg-1*$^{fl/fl}$;*Tie-2*^{null} (WT) or *Arg-1*$^{fl/fl}$;*Tie-2*^{Cre} mice (A to C) or in C57BL/6 mice (D to F), whereupon animals received daily treatments of apocynin (6 mg/kg) (A to C), L-NIL (40 mg/kg) (A to C), or DFMO (50 mg/kg) (D to F) beginning 5 h prior to infection. Bacterial burdens in surrounding soft tissues (A and D), the femur (B and E), and the knee joint (C and F) were quantified at the indicated time points postinfection. *, $P < 0.05$; ***, $P < 0.001$ (unpaired 2-tailed Student's *t* test).

neuronal NOS (nNOS) and endothelial NOS (eNOS) (42). Both *Arg-1*$^{fl/fl}$;*Tie-2*^{Cre} myeloid conditional KO and *Arg-1*$^{fl/fl}$;*Tie-2*^{null} control mice received daily administration of L-NIL or vehicle in the *S. aureus* orthopedic implant model. No significant differences in bacterial burdens from the knee, surrounding soft tissue, femur, or leukocyte infiltrates were observed with L-NIL treatment (Fig. 5A to C and data not shown), suggesting that the observed increase in iNOS expression by MDSCs does not compensate for reduced myeloid Arg-1. We next examined the potential role of NADPH oxidase as a redundant pathway for Arg-1 in modulating biofilm persistence, since reactive oxygen species (ROS) production by MDSCs has also been implicated in modulating their suppressive activity (43, 44). *Arg-1*$^{fl/fl}$;*Tie-2*^{Cre} myeloid conditional KO and *Arg-1*$^{fl/fl}$;*Tie-2*^{null} control mice were treated with the small-molecule NADPH oxidase inhibitor apocynin, which also revealed no role in limiting the establishment or persistence of orthopedic implant-associated biofilm infection (Fig. 5A to C).

Inhibition of polyamine synthesis promotes bacterial growth in tissues surrounding biofilm infections. Although our results suggested that myeloid Arg-1 deletion had minimal effects on biofilm development, we treated WT mice with difluoromethylornithine (DFMO), a small-molecule inhibitor of both arginase and ornithine decarboxylase (ODC), in the orthopedic implant infection model to examine the potential redundancy of ODC during *S. aureus* biofilm infection. Interestingly, bacterial burdens were increased at days 7 and 10 postinfection with DFMO treatment but were manifest only in the soft tissue surrounding the biofilm infection site (Fig. 5D). This finding agrees with an earlier report showing that polyamines are critical for antistaphylococcal responses and resolution of skin abscesses following DFMO treatment (31). Importantly, our study advances this finding by identifying myeloid cells as a critical source of Arg-1 during subcutaneous *S. aureus* abscess formation, since bacterial burdens were significantly increased in abscesses from *Arg-1*$^{fl/fl}$;*Tie-2*^{Cre} mice compared to those from WT mice (Fig. 6A). No gross differences in abscess size or dermatonecrosis

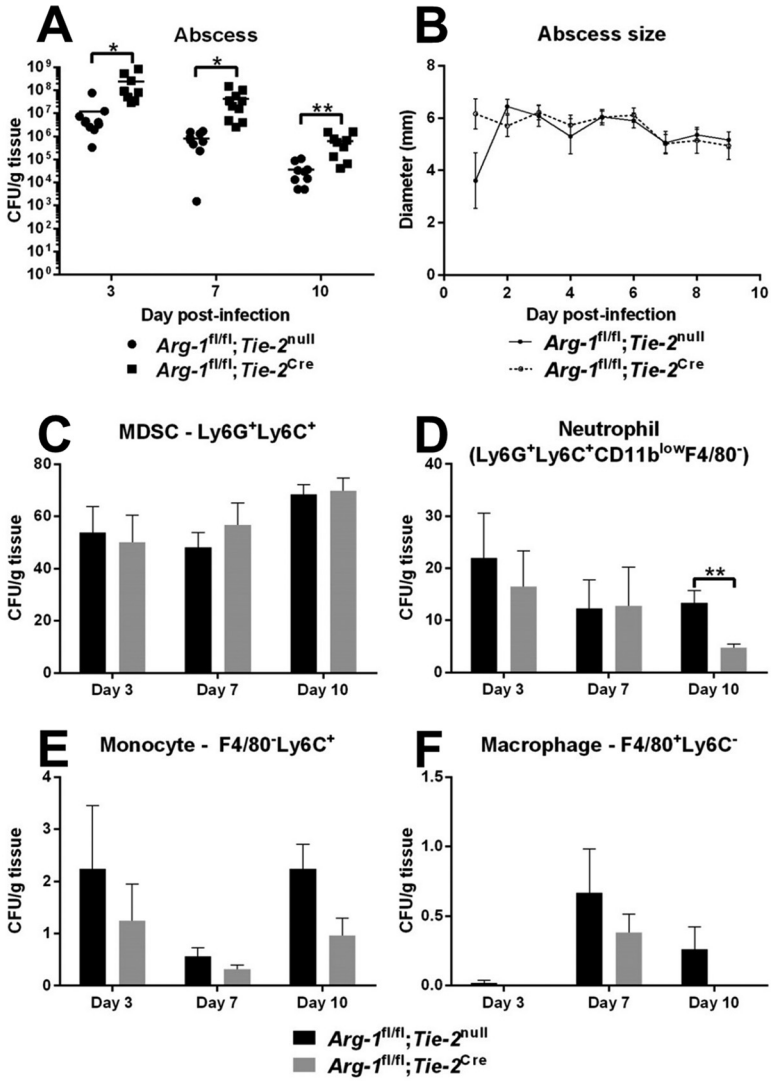

FIG 6 Myeloid-derived arginase-1 contributes to *S. aureus* clearance during subcutaneous abscess infection. Subcutaneous abscesses were established in *Arg-1*$^{fl/fl}$;*Tie-2*^{null} (WT) and *Arg-1*$^{fl/fl}$;*Tie-2*^{Cre} mice following inoculation with 10^7 CFU *S. aureus* LAC. Animals were sacrificed at days 3, 7, and 10 postinfection, whereupon abscess-associated bacterial burdens (A) and leukocyte infiltrates (C to F) were measured. (B) Abscess sizes were monitored by use of calipers throughout the course of infection. Results are representative of two independent experiments. *, $P < 0.05$; **, $P < 0.01$ (unpaired 2-tailed Student's *t* test).

were observed between *Arg-1*$^{fl/fl}$;*Tie-2*^{Cre} myeloid conditional KO and *Arg-1*$^{fl/fl}$;*Tie-2*^{null} control mice (Fig. 6B and data not shown). We did not explore the effects of DFMO on MDSC function, since our data demonstrated that myeloid-derived Arg-1 does not play a major role during *S. aureus* biofilm formation. Collectively, these results demonstrate that myeloid-derived Arg-1 controls *S. aureus* growth during planktonic but not biofilm growth *in vivo*.

DISCUSSION

Our laboratory has demonstrated that MDSCs are preferentially recruited to *S. aureus* biofilm infections, where they inhibit monocyte proinflammatory activity to promote infection persistence (10, 12–16). MDSCs are the primary source of IL-10 during biofilm infection, and prior studies have established that antibody-mediated depletion of MDSCs and IL-10 deficiency both result in reduced *S. aureus* biofilm burdens (10, 12, 14, 16). However, bacteria still remain in implant-associated tissues in

both of these scenarios, indicating the existence of additional immunosuppressive mechanisms. Previous reports have shown that MDSCs and macrophages inhibit innate and adaptive immune responses through extracellular arginine depletion by Arg-1 (23, 26, 45). Our recent studies revealed that Arg-1 expression is increased in MDSCs during *S. aureus* orthopedic implant biofilm infection and that macrophages surrounding biofilm-infected catheters dramatically upregulate Arg-1 (10–12, 14). Furthermore, host polyamine synthesis is important for controlling *S. aureus* growth in nonbiofilm infection models, such as models of sepsis and subcutaneous abscesses (31). Arg-1 also plays a critical role in models of cancer, Alzheimer's disease, and infection because of its immunosuppressive properties (18, 24, 35, 36). Based on these observations, we sought to determine whether myeloid-derived Arg-1 facilitates *S. aureus* biofilm persistence, which may represent a viable treatment target since the enzyme is currently being explored as a therapeutic target in Alzheimer's disease (35).

Despite efficient depletion of myeloid-derived arginase activity from *Arg-1*$^{fl/fl}$;*Tie-2*^{Cre} mice, minimal differences in bacterial burdens or leukocyte infiltrates were observed in two distinct *S. aureus* device-associated biofilm infection models. MDSCs are the primary leukocyte infiltrate in both orthopedic implant and catheter-associated biofilm infections, whereas fewer T cells and neutrophils are present. However, one important distinction is that macrophage infiltrates are more abundant in catheter-associated infections than in the orthopedic implant model (10, 12–14). The finding that leukocyte infiltrates were similar in *Arg-1*$^{fl/fl}$;*Tie-2*^{Cre} myeloid conditional KO and *Arg-1*$^{fl/fl}$;*Tie-2*^{null} control mice in both models supports previous reports that Arg-1 activity regulates cellular activation rather than differential leukocyte recruitment (18, 23–25, 27). However, cellular activation status was not examined in the current study, since no dramatic differences in biofilm titers were observed.

Interestingly, a marked increase in iNOS expression was observed in MDSCs from *Arg-1*$^{fl/fl}$;*Tie-2*^{Cre} myeloid conditional KO animals both 7 and 14 days following infection. A previous study reported a similar phenomenon, where deletion of macrophage Arg-1 potentiated NO production by increasing arginine availability (24). To determine whether this increase in iNOS expression could compensate for myeloid-targeted Arg-1 depletion, *Arg-1*$^{fl/fl}$;*Tie-2*^{Cre} mice were treated with L-NIL, a small-molecule inhibitor of iNOS. L-NIL had no effect on biofilm burdens or leukocyte infiltrates in *Arg-1*$^{fl/fl}$;*Tie-2*^{Cre} myeloid conditional KO mice, indicating that increased iNOS expression is not a significant compensatory mechanism for promoting biofilm persistence. In addition, unpublished data from our laboratory, using iNOS KO mice, demonstrated that iNOS does not play a role in *S. aureus* biofilm infections. In contrast, McInnes et al. reported increased bacterial burdens and mortality during *S. aureus* septic arthritis in iNOS KO mice (46), identifying a distinction between biofilm and planktonic infections. In addition, the current study demonstrates that NADPH does not have an impact on biofilm growth, since apocynin treatment had no effect on *S. aureus* burdens. This differs from the results of a recent study of NADPH oxidase-deficient mice by Sun et al., which revealed a critical role for ROS in controlling *S. aureus* pneumonia (47). Therefore, our study has revealed novel distinctions between *S. aureus* biofilm and planktonic infections, since iNOS and NADPH oxidase do not affect biofilm formation but do regulate host immunity to planktonic infection.

As another potential point of redundancy, we examined whether ODC contributes to *S. aureus* persistence during biofilm infection, since a prior report revealed a critical role for polyamine synthesis in controlling *S. aureus* growth in a mouse skin abscess model (31). Interestingly, treatment of WT animals with the arginase/ODC inhibitor DFMO increased bacterial burdens in the soft tissue surrounding infected orthopedic implants at days 7 and 10 postinfection, whereas no changes in bacterial titers were observed in the knee joint, femur, or implant. The selectivity of DFMO action in the tissue is reminiscent of our findings with the catheter-associated infection model, in which *S. aureus* burdens in *Arg-1*$^{fl/fl}$;*Tie-2*^{Cre} conditional KO mice at day 10 postinfection were elevated in the surrounding soft tissues, which possess some attributes of a planktonic environment since bacteria have dispersed from the catheter surface. To

further demonstrate the importance of Arg-1 in the context of planktonic infection, we took advantage of a subcutaneous abscess model in which a role for polyamines in controlling bacterial growth was previously shown (31). Importantly, our study advances this finding by identifying myeloid cells as a critical source of Arg-1 during subcutaneous *S. aureus* abscess formation, since bacterial burdens were significantly increased in abscesses from *Arg-1*$^{fl/fl}$;*Tie-2*^{Cre} mice compared to those in WT mice. Collectively, these results demonstrate that myeloid-derived Arg-1 activity and polyamine synthesis control *S. aureus* growth during planktonic but not biofilm growth *in vivo*.

The complete repertoire of mechanisms used by MDSCs to inhibit immune function and promote *S. aureus* biofilm establishment and persistence is still unknown. Previous studies from our laboratory implicated roles for IL-12 and IL-10 in the indirect recruitment and immunosuppressive function of MDSCs, respectively (12, 13). In cancer models, myeloid-derived Arg-1 has been shown to provide two complementary functions. First, depletion of extracellular arginine stores modulates the immune response by decreasing NO production, synthesis of arginine-containing proteins, and T cell activation (18, 29, 30, 48). Second, arginine metabolism provides precursor molecules for collagen and polyamine synthesis, which leads to fibrotic tissue deposition, vascular remodeling, and direct antibacterial actions (23, 28–31, 39). Although prior work suggested that myeloid Arg-1 might be important for promoting *S. aureus* biofilm infection (12–14), the present study demonstrates that myeloid Arg-1 does not directly influence the immune response to *S. aureus* biofilm infections or induce a compensatory increase in arginine flux toward reactive nitrogen intermediate (RNI)/ROS production. However, these observations do not provide a specific mechanism by which this occurs. Namely, they do not rule out potential effects of Arg-1 on arginine bioavailability to support *S. aureus* growth and fitness *in vivo*. For example, previous studies demonstrated that *S. aureus* growth and virulence are dependent on exogenous arginine or arginine biosynthesis via proline (49). Alternatively, *S. aureus* biofilm induction of Arg-1 expression in nonmyeloid cells, such as fibroblasts or other mesenchymal cells, may override any potential contribution of myeloid-derived Arg-1 activity during *S. aureus* biofilm infection. This would require crossing of an *Arg-1*$^{fl/fl}$ line with a Cre line directed by the type I collagen promoter Col1a2 to target gene deletion in fibroblasts (50). Furthermore, mitochondrial Arg-2 released from dead or dying cells may also contribute to the overall pool of arginase enzyme activity (41). Additional studies are needed to address these possibilities; however, the present study demonstrates that myeloid-derived Arg-1 has minimal effects on *S. aureus* biofilm growth but instead plays a unique role in controlling *S. aureus* planktonic infections.

MATERIALS AND METHODS

Mice. Male and female C57BL/6 mice (8 weeks of age) were purchased from The Jackson Laboratory (Bar Harbor, ME, USA). *Arg-1*$^{fl/fl}$;*Tie-2*^{Cre} and *Arg-1*$^{fl/fl}$;*LysM*^{Cre} mice were generated by crossing *Arg-1*$^{fl/fl}$ animals with *Tie-2*^{Cre} and *LysM*^{Cre} animals, respectively, both on a C57BL/6 background (The Jackson Laboratory), with *Arg-1*$^{fl/fl}$ littermates used as WT controls. This study was conducted in strict accordance with the recommendations in the *Guide for the Care and Use of Laboratory Animals* (51). The animal protocol was approved by the Institutional Animal Care and Use Committee of the University of Nebraska Medical Center.

Generation of bone marrow-derived macrophages. Macrophages were expanded from the bone marrow of *Arg-1*$^{fl/fl}$;*Tie-2*^{Cre} conditional KO, *Arg-1*$^{fl/fl}$;*LysM*^{Cre}, and *Arg-1*$^{fl/fl}$;*Tie-2*^{null} control mice by flushing long bones with sterile RPMI 1640 serum-free medium and culturing cells in RPMI 1640 medium containing 10% fetal bovine serum (FBS) (Atlanta Biologicals, Atlanta, GA), penicillin-streptomycin-amphotericin B (Fungizone), and 5% conditioned medium from L929 fibroblasts as a source of macrophage colony-stimulating factor (M-CSF) (11, 52). FACS analysis revealed that >99% of cells were macrophages, based on CD11b and F4/80 staining, after a 6-day culture period (data not shown). At *in vitro* day 6, macrophages were harvested, replated, and treated with 10 ng/ml recombinant mouse IL-4 (rmIL-4) (BioLegend, San Diego, CA) for 24 h, whereupon cellular extracts were prepared for Western blotting and Arg-1 activity assays. Western blotting was performed as previously described (53), with an anti-Arg-1 antibody (goat anti-mouse; 1:200) (sc-271430; Santa Cruz Biotechnology) followed by a rabbit anti-goat IgG conjugated to horseradish peroxidase (HRP) (Abcam, Cambridge, MA). Arginase activity in macrophages was measured using an arginase activity assay kit (Sigma-Aldrich, St. Louis, MO).

Mouse models of device-associated *S. aureus* biofilm infection. Mouse models of *S. aureus* catheter-associated and orthopedic implant biofilm infections were performed as previously described (10–13, 15, 17). Briefly, for both device-associated models, mice were anesthetized with ketamine-xylazine (100 mg/kg of body weight-5 mg/kg of body weight), and the surgical site was disinfected with povidone-iodine. The health status of mice was regularly monitored throughout the course of infection, and all mice exhibited normal ambulation and no discernible pain behaviors. *S. aureus* catheter-associated biofilm infections were performed as previously described (10, 15, 16). Briefly, a 1-cm subcutaneous incision was made in the flank, and a blunt probe was used to create a pocket for insertion of a 1-cm sterile 16-gauge Teflon-coated intravenous (i.v.) catheter (Excel International, St. Petersburg, FL). The incision was sealed using Vetbond tissue adhesive (3M, St. Paul, MN), whereupon a total of 10^3 CFU of *S. aureus* USA300 LAC (54) in 20 μl 1$\times$ phosphate-buffered saline (PBS) was injected directly into the catheter lumen to establish biofilm formation.

To model infectious complications that can arise in patients following arthroplasty, a mouse model of *S. aureus* orthopedic implant infection was used as previously described (12–14, 17, 55). Briefly, after a surgical plane of ketamine-xylazine anesthesia was achieved, a medial incision was created through the quadriceps, with lateral displacement to access the distal femur. A burr hole was made in the femoral intercondylar notch through the intramedullary canal, using a 26-gauge needle, whereupon a precut 0.8-cm orthopedic-grade Kirschner wire (0.6-mm diameter) (Nitinol [nickel-titanium]; Custom Wire Technologies, Port Washington, WI) was inserted into the intramedullary canal, leaving ~1 mm protruding into the joint space. The exposed wire surface was inoculated with 10^3 CFU of *S. aureus* USA300 LAC in 2 μl of 1$\times$ PBS. Following closure of the surgical site with absorbable nylon sutures, animals received s.c. buprenorphine (Buprenex) (0.1 mg/kg; Reckitt Benckiser, Hull, United Kingdom) for the first 24 h after surgery for pain relief. Detailed time course studies were initiated for the catheter-associated model, with mice sacrificed on days 3, 5, 7, and 10 postinfection. Subsequent studies were conducted with a more limited set of time points in the orthopedic infection model, with mice analyzed at days 3, 7, and 14 postinfection.

Mouse model of *S. aureus* abscess infection. *S. aureus* subcutaneous abscesses were induced as previously described (31, 49). Briefly, *Arg-1*$^{fl/fl}$*;Tie-2*^{Cre} conditional KO and *Arg-1*$^{fl/fl}$*;Tie-2*^{null} control mice were anesthetized with ketamine-xylazine (100 mg/kg-5 mg/kg), the flank was shaved using clippers, and the surgical site was disinfected with povidone-iodine. Mice received subcutaneous injections of *S. aureus* (10^7 CFU in 20 μl PBS), and abscess sizes were measured daily by use of calipers throughout the course of infection. Mice were euthanized at days 3, 7, and 10 postinfection to quantify bacterial burdens and leukocyte infiltrates.

Recovery of infected tissues for *S. aureus* enumeration. The soft tissue surrounding catheter-associated infections was collected, weighed, and dissociated using the blunt end of a 3.0-ml syringe in 500 μl of PBS supplemented with a protease inhibitor cocktail tablet (Roche Diagnostics, Indianapolis, IN). Catheters were placed in 500 μl of PBS for sonication to dissociate bacteria from the catheter surface. For the orthopedic implant infection model, the titanium implant, femur, knee joint, and surrounding soft tissue were collected by first removing the skin, whereupon the tissue ventral to the patellar tendon was excised, weighed, and disrupted using the blunt end of a 3.0-ml syringe in 500 μl of PBS supplemented with a protease inhibitor cocktail tablet. The remaining muscle and tendons were removed and excluded from analysis. The knee joint and femur were separated and homogenized individually by use of a hand-held homogenizer for 30 s. The titanium implant was carefully removed and vortexed in 200 μl PBS to dislodge biofilm-associated bacteria. Subcutaneous abscesses were collected, weighed, and dissociated using the blunt end of a 3.0-ml syringe in 500 μl of PBS. *S. aureus* titers were quantified using tryptic soy agar (TSA) plates supplemented with 5% sheep blood (Remel, Lenexa, KS) and are expressed as CFU per milliliter for catheters/titanium implants or CFU per gram of wet tissue weight.

Flow cytometry. To characterize leukocyte infiltrates associated with soft tissues surrounding the infected knee, catheter, or abscess, homogenates were passed through a 35-μm filter (BD Falcon, BD Biosciences). The cellular filtrate was washed with PBS supplemented with 2% heat-inactivated FBS and collected by centrifugation (300 $\times$ *g*, 5 min), whereupon red blood cells (RBCs) were lysed using RBC lysis buffer (BioLegend, San Diego, CA). Cells were washed and resuspended in PBS containing 2% FBS and then incubated with TruStain fcX (BioLegend, San Diego, CA) to minimize nonspecific antibody binding. Cells were then stained with Live/Dead Fixable Blue dead cell stain (Invitrogen, Eugene, OR), CD45-allophycocyanin (CD45-APC), Ly6G-phycoerythrin (Ly6G-PE), Ly6C-peridinin chlorophyll protein (PerCP)-Cy5.5, and F4/80-PE-Cy7 (BioLegend, San Diego, CA). An aliquot of pooled cells was stained with isotype-matched control Abs to assess the degree of nonspecific staining per treatment group. For individual samples, 10,000 to 100,000 events were analyzed using BD FACSDiva software, with cell populations expressed as percentages of total viable CD45$^+$ leukocytes.

Hydroxyproline assay. To determine the relative collagen content in infected tissues, hydroxyproline assays were performed using a hydroxyproline assay kit (Sigma-Aldrich). Briefly, samples were prepared by homogenization of 10 mg of infected tissue in 100 μl of water, transferred to a pressure-tight vial with 100 μl of 12 M hydrochloric acid, and hydrolyzed at 120°C for 3 h. A total of 10 to 50 μl per sample was transferred to a 96-well plate and evaporated at 60°C. Following the addition of reaction buffer, the plate was read at 570 nm by use of an iMark microplate absorbance reader (Bio-Rad, Hercules, CA).

Statistics. Significant differences between experimental groups were determined by an unpaired two-tailed Student *t* test or one-way analysis of variance (ANOVA) with Bonferroni's multiple-comparison test, using GraphPad Prism 6 (GraphPad Software, La Jolla, CA). For all analyses, *P* values of <0.05 were considered statistically significant.

SUPPLEMENTAL MATERIAL

Supplemental material for this article may be found at https://doi.org/10.1128/IAI.00206-18.

SUPPLEMENTAL FILE 1, PDF file, 0.3 MB.

ACKNOWLEDGMENTS

This work was supported by the NIH National Institute of Allergy and Infectious Diseases (NIAID) under grant 2P01AI083211 (project 4 to T.K.).

We thank Rachel Fallet for managing the mouse colony and Craig Semerad, Victoria Smith, and Samantha Wall of the UNMC Flow Cytometry Core Facility for assistance with FACS analysis.

REFERENCES

1. Fowler VG, Jr, Olsen MK, Corey GR, Woods CW, Cabell CH, Reller LB, Cheng AC, Dudley T, Oddone EZ. 2003. Clinical identifiers of complicated Staphylococcus aureus bacteremia. Arch Intern Med 163:2066–2072. https://doi.org/10.1001/archinte.163.17.2066.
2. Morgenstern M, Erichsen C, Hackl S, Mily J, Militz M, Friederichs J, Hungerer S, Buhren V, Moriarty TF, Post V, Richards RG, Kates SL. 2016. Antibiotic resistance of commensal Staphylococcus aureus and coagulase-negative staphylococci in an international cohort of surgeons: a prospective point-prevalence study. PLoS One 11:e0148437. https://doi.org/10.1371/journal.pone.0148437.
3. Naber CK. 2009. Staphylococcus aureus bacteremia: epidemiology, pathophysiology, and management strategies. Clin Infect Dis 48(Suppl 4):S231–S237. https://doi.org/10.1086/598189.
4. Walls RJ, Roche SJ, O'Rourke A, McCabe JP. 2008. Surgical site infection with methicillin-resistant Staphylococcus aureus after primary total hip replacement. J Bone Joint Surg Br 90:292–298. https://doi.org/10.1302/0301-620X.90B3.20155.
5. Self WH, Wunderink RG, Williams DJ, Zhu Y, Anderson EJ, Balk RA, Fakhran SS, Chappell JD, Casimir G, Courtney DM, Trabue C, Waterer GW, Bramley A, Magill S, Jain S, Edwards KM, Grijalva CG. 2016. Staphylococcus aureus community-acquired pneumonia: prevalence, clinical characteristics, and outcomes. Clin Infect Dis 63:300–309. https://doi.org/10.1093/cid/ciw300.
6. Tande AJ, Osmon DR, Greenwood-Quaintance KE, Mabry TM, Hanssen AD, Patel R. 2014. Clinical characteristics and outcomes of prosthetic joint infection caused by small colony variant staphylococci. mBio 5:e01910-14. https://doi.org/10.1128/mBio.01910-14.
7. Tande AJ, Patel R. 2014. Prosthetic joint infection. Clin Microbiol Rev 27:302–345. https://doi.org/10.1128/CMR.00111-13.
8. Guggenbichler JP, Assadian O, Boeswald M, Kramer A. 2011. Incidence and clinical implication of nosocomial infections associated with implantable biomaterials—catheters, ventilator-associated pneumonia, urinary tract infections. GMS Krankenhhyg Interdiszip 6:Doc18. https://doi.org/10.3205/dgkh000175.
9. Klein E, Smith DL, Laxminarayan R. 2007. Hospitalizations and deaths caused by methicillin-resistant Staphylococcus aureus, United States, 1999–2005. Emerg Infect Dis 13:1840–1846. https://doi.org/10.3201/eid1312.070629.
10. Hanke ML, Heim CE, Angle A, Sanderson SD, Kielian T. 2013. Targeting macrophage activation for the prevention and treatment of Staphylococcus aureus biofilm infections. J Immunol 190:2159–2168. https://doi.org/10.4049/jimmunol.1202348.
11. Hanke ML, Kielian T. 2012. Deciphering mechanisms of staphylococcal biofilm evasion of host immunity. Front Cell Infect Microbiol 2:62. https://doi.org/10.3389/fcimb.2012.00062.
12. Heim CE, Vidlak D, Kielian T. 2015. Interleukin-10 production by myeloid-derived suppressor cells contributes to bacterial persistence during Staphylococcus aureus orthopedic biofilm infection. J Leukoc Biol 98:1003–1013. https://doi.org/10.1189/jlb.4VMA0315-125RR.
13. Heim CE, Vidlak D, Scherr TD, Hartman CW, Garvin KL, Kielian T. 2015. IL-12 promotes myeloid-derived suppressor cell recruitment and bacterial persistence during Staphylococcus aureus orthopedic implant infection. J Immunol 194:3861–3872. https://doi.org/10.4049/jimmunol.1402689.
14. Heim CE, Vidlak D, Scherr TD, Kozel JA, Holzapfel M, Muirhead DE, Kielian T. 2014. Myeloid-derived suppressor cells contribute to Staphylococcus aureus orthopedic biofilm infection. J Immunol 192:3778–3792. https://doi.org/10.4049/jimmunol.1303408.
15. Thurlow LR, Hanke ML, Fritz T, Angle A, Aldrich A, Williams SH, Engebretsen IL, Bayles KW, Horswill AR, Kielian T. 2011. Staphylococcus aureus biofilms prevent macrophage phagocytosis and attenuate inflammation in vivo. J Immunol 186:6585–6596. https://doi.org/10.4049/jimmunol.1002794.
16. Hanke ML, Angle A, Kielian T. 2012. MyD88-dependent signaling influences fibrosis and alternative macrophage activation during Staphylococcus aureus biofilm infection. PLoS One 7:e42476. https://doi.org/10.1371/journal.pone.0042476.
17. Heim CE, Hanke ML, Kielian T. 2014. A mouse model of Staphylococcus catheter-associated biofilm infection. Methods Mol Biol 1106:183–191. https://doi.org/10.1007/978-1-62703-736-5_17.
18. Munder M. 2009. Arginase: an emerging key player in the mammalian immune system. Br J Pharmacol 158:638–651. https://doi.org/10.1111/j.1476-5381.2009.00291.x.
19. Makarenkova VP, Bansal V, Matta BM, Perez LA, Ochoa JB. 2006. CD11b+/Gr-1+ myeloid suppressor cells cause T cell dysfunction after traumatic stress. J Immunol 176:2085–2094. https://doi.org/10.4049/jimmunol.176.4.2085.
20. Rodriguez PC, Quiceno DG, Ochoa AC. 2007. L-Arginine availability regulates T-lymphocyte cell-cycle progression. Blood 109:1568–1573. https://doi.org/10.1182/blood-2006-06-031856.
21. Rodriguez PC, Zea AH, DeSalvo J, Culotta KS, Zabaleta J, Quiceno DG, Ochoa JB, Ochoa AC. 2003. L-Arginine consumption by macrophages modulates the expression of CD3 zeta chain in T lymphocytes. J Immunol 171:1232–1239. https://doi.org/10.4049/jimmunol.171.3.1232.
22. Zhu X, Pribis JP, Rodriguez PC, Morris SM, Jr, Vodovotz Y, Billiar TR, Ochoa JB. 2014. The central role of arginine catabolism in T-cell dysfunction and increased susceptibility to infection after physical injury. Ann Surg 259:171–178. https://doi.org/10.1097/SLA.0b013e31828611f8.
23. Bronte V, Serafini P, De Santo C, Marigo I, Tosello V, Mazzoni A, Segal DM, Staib C, Lowel M, Sutter G, Colombo MP, Zanovello P. 2003. IL-4-induced arginase 1 suppresses alloreactive T cells in tumor-bearing mice. J Immunol 170:270–278. https://doi.org/10.4049/jimmunol.170.1.270.
24. El Kasmi KC, Qualls JE, Pesce JT, Smith AM, Thompson RW, Henao-Tamayo M, Basaraba RJ, Konig T, Schleicher U, Koo MS, Kaplan G, Fitzgerald KA, Tuomanen EI, Orme IM, Kanneganti TD, Bogdan C, Wynn TA, Murray PJ. 2008. Toll-like receptor-induced arginase 1 in macrophages thwarts effective immunity against intracellular pathogens. Nat Immunol 9:1399–1406. https://doi.org/10.1038/ni.1671.
25. Modolell M, Choi BS, Ryan RO, Hancock M, Titus RG, Abebe T, Hailu A, Muller I, Rogers ME, Bangham CR, Munder M, Kropf P. 2009. Local suppression of T cell responses by arginase-induced L-arginine depletion in nonhealing leishmaniasis. PLoS Negl Trop Dis 3:e480. https://doi.org/10.1371/journal.pntd.0000480.
26. Rodriguez PC, Quiceno DG, Zabaleta J, Ortiz B, Zea AH, Piazuelo MB, Delgado A, Correa P, Brayer J, Sotomayor EM, Antonia S, Ochoa JB, Ochoa AC. 2004. Arginase I production in the tumor microenvironment by mature myeloid cells inhibits T-cell receptor expression and antigen-specific T-cell responses. Cancer Res 64:5839–5849. https://doi.org/10.1158/0008-5472.CAN-04-0465.
27. Wijnands KA, Hoeksema MA, Meesters DM, van den Akker NM, Molin DG,

Briede JJ, Ghosh M, Kohler SE, van Zandvoort MA, de Winther MP, Buurman WA, Lamers WH, Poeze M. 2014. Arginase-1 deficiency regulates arginine concentrations and NOS2-mediated NO production during endotoxemia. PLoS One 9:e86135. https://doi.org/10.1371/journal.pone.0086135.
28. Gaur U, Roberts SC, Dalvi RP, Corraliza I, Ullman B, Wilson ME. 2007. An effect of parasite-encoded arginase on the outcome of murine cutaneous leishmaniasis. J Immunol 179:8446–8453. https://doi.org/10.4049/jimmunol.179.12.8446.
29. Maarsingh H, Leusink J, Bos IS, Zaagsma J, Meurs H. 2006. Arginase strongly impairs neuronal nitric oxide-mediated airway smooth muscle relaxation in allergic asthma. Respir Res 7:6. https://doi.org/10.1186/1465-9921-7-6.
30. Meurs H, McKay S, Maarsingh H, Hamer MA, Macic L, Molendijk N, Zaagsma J. 2002. Increased arginase activity underlies allergen-induced deficiency of cNOS-derived nitric oxide and airway hyperresponsiveness. Br J Pharmacol 136:391–398. https://doi.org/10.1038/sj.bjp.0704725.
31. Thurlow LR, Joshi GS, Clark JR, Spontak JS, Neely CJ, Maile R, Richardson AR. 2013. Functional modularity of the arginine catabolic mobile element contributes to the success of USA300 methicillin-resistant Staphylococcus aureus. Cell Host Microbe 13:100–107. https://doi.org/10.1016/j.chom.2012.11.012.
32. Zabaleta J, McGee DJ, Zea AH, Hernandez CP, Rodriguez PC, Sierra RA, Correa P, Ochoa AC. 2004. Helicobacter pylori arginase inhibits T cell proliferation and reduces the expression of the TCR zeta-chain (CD3zeta). J Immunol 173:586–593. https://doi.org/10.4049/jimmunol.173.1.586.
33. Bian Z, Abdelaal AM, Shi L, Liang H, Xiong L, Kidder K, Venkataramani M, Culpepper C, Zen K, Liu Y. 28 February 2018. Arginase-1 is neither constitutively expressed in nor required for myeloid-derived suppressor cell-mediated inhibition of T-cell proliferation. Eur J Immunol https://doi.org/10.1002/eji.201747355.
34. Deshane J, Zmijewski JW, Luther R, Gaggar A, Deshane R, Lai JF, Xu X, Spell M, Estell K, Weaver CT, Abraham E, Schwiebert LM, Chaplin DD. 2011. Free radical-producing myeloid-derived regulatory cells: potent activators and suppressors of lung inflammation and airway hyperresponsiveness. Mucosal Immunol 4:503–518. https://doi.org/10.1038/mi.2011.16.
35. Kan MJ, Lee JE, Wilson JG, Everhart AL, Brown CM, Hoofnagle AN, Jansen M, Vitek MP, Gunn MD, Colton CA. 2015. Arginine deprivation and immune suppression in a mouse model of Alzheimer's disease. J Neurosci 35:5969–5982. https://doi.org/10.1523/JNEUROSCI.4668-14.2015.
36. Knippenberg S, Brumshagen C, Aschenbrenner F, Welte T, Maus UA. 2015. Arginase 1 activity worsens lung-protective immunity against Streptococcus pneumoniae infection. Eur J Immunol 45:1716–1726. https://doi.org/10.1002/eji.201445419.
37. Kisanuki YY, Hammer RE, Miyazaki J, Williams SC, Richardson JA, Yanagisawa M. 2001. Tie2-Cre transgenic mice: a new model for endothelial cell-lineage analysis in vivo. Dev Biol 230:230–242. https://doi.org/10.1006/dbio.2000.0106.
38. Fletcher M, Ramirez ME, Sierra RA, Raber P, Thevenot P, Al-Khami AA, Sanchez-Pino D, Hernandez C, Wyczechowska DD, Ochoa AC, Rodriguez PC. 2015. L-Arginine depletion blunts antitumor T-cell responses by inducing myeloid-derived suppressor cells. Cancer Res 75:275–283. https://doi.org/10.1158/0008-5472.CAN-14-1491.
39. Geeraerts X, Bolli E, Fendt SM, Van Ginderachter JA. 2017. Macrophage metabolism as therapeutic target for cancer, atherosclerosis, and obesity. Front Immunol 8:289. https://doi.org/10.3389/fimmu.2017.00289.
40. Murray PJ, Wynn TA. 2011. Obstacles and opportunities for understanding macrophage polarization. J Leukoc Biol 89:557–563. https://doi.org/10.1189/jlb.0710409.
41. Choi S, Park C, Ahn M, Lee JH, Shin T. 2012. Immunohistochemical study of arginase 1 and 2 in various tissues of rats. Acta Histochem 114:487–494. https://doi.org/10.1016/j.acthis.2011.09.002.
42. Grant SK, Green BG, Stiffey-Wilusz J, Durette PL, Shah SK, Kozarich JW. 1998. Structural requirements for human inducible nitric oxide synthase substrates and substrate analogue inhibitors. Biochemistry 37:4174–4180. https://doi.org/10.1021/bi972481d.
43. Gabrilovich DI, Nagaraj S. 2009. Myeloid-derived suppressor cells as regulators of the immune system. Nat Rev Immunol 9:162–174. https://doi.org/10.1038/nri2506.
44. Gabrilovich DI, Ostrand-Rosenberg S, Bronte V. 2012. Coordinated regulation of myeloid cells by tumours. Nat Rev Immunol 12:253–268. https://doi.org/10.1038/nri3175.
45. Kusmartsev S, Gabrilovich DI. 2003. Inhibition of myeloid cell differentiation in cancer: the role of reactive oxygen species. J Leukoc Biol 74:186–196. https://doi.org/10.1189/jlb.0103010.
46. McInnes IB, Leung B, Wei XQ, Gemmell CC, Liew FY. 1998. Septic arthritis following Staphylococcus aureus infection in mice lacking inducible nitric oxide synthase. J Immunol 160:308–315.
47. Sun K, Yajjala VK, Bauer C, Talmon GA, Fischer KJ, Kielian T, Metzger DW. 2016. Nox2-derived oxidative stress results in inefficacy of antibiotics against post-influenza S. aureus pneumonia. J Exp Med 213:1851–1864. https://doi.org/10.1084/jem.20150514.
48. Bronte V, Brandau S, Chen SH, Colombo MP, Frey AB, Greten TF, Mandruzzato S, Murray PJ, Ochoa A, Ostrand-Rosenberg S, Rodriguez PC, Sica A, Umansky V, Vonderheide RH, Gabrilovich DI. 2016. Recommendations for myeloid-derived suppressor cell nomenclature and characterization standards. Nat Commun 7:12150. https://doi.org/10.1038/ncomms12150.
49. Nuxoll AS, Halouska SM, Sadykov MR, Hanke ML, Bayles KW, Kielian T, Powers R, Fey PD. 2012. CcpA regulates arginine biosynthesis in Staphylococcus aureus through repression of proline catabolism. PLoS Pathog 8:e1003033. https://doi.org/10.1371/journal.ppat.1003033.
50. Zheng B, Zhang Z, Black CM, de Crombrugghe B, Denton CP. 2002. Ligand-dependent genetic recombination in fibroblasts: a potentially powerful technique for investigating gene function in fibrosis. Am J Pathol 160:1609–1617. https://doi.org/10.1016/S0002-9440(10)61108-X.
51. National Research Council. 2011. Guide for the care and use of laboratory animals, 8th ed. National Academies Press, Washington, DC.
52. Kigerl KA, Gensel JC, Ankeny DP, Alexander JK, Donnelly DJ, Popovich PG. 2009. Identification of two distinct macrophage subsets with divergent effects causing either neurotoxicity or regeneration in the injured mouse spinal cord. J Neurosci 29:13435–13444. https://doi.org/10.1523/JNEUROSCI.3257-09.2009.
53. Aldrich A, Kielian T. 2011. Central nervous system fibrosis is associated with fibrocyte-like infiltrates. Am J Pathol 179:2952–2962. https://doi.org/10.1016/j.ajpath.2011.08.036.
54. DeLeo FR, Otto M, Kreiswirth BN, Chambers HF. 2010. Community-associated meticillin-resistant Staphylococcus aureus. Lancet 375:1557–1568. https://doi.org/10.1016/S0140-6736(09)61999-1.
55. Scherr TD, Lindgren KE, Schaeffer CR, Hanke ML, Hartman CW, Kielian T. 2014. Mouse model of post-arthroplasty Staphylococcus epidermidis joint infection. Methods Mol Biol 1106:173–181. https://doi.org/10.1007/978-1-62703-736-5_16.